

Article

A New Method for Preparing Titanium Aluminium Alloy Powder

Jialong Kang^{1,2}, Yaoran Cui^{1,2}, Dapeng Zhong^{1,2}, Guibao Qiu^{1,2,*} and Xuewei Lv^{1,2}

¹ Chongqing Key Laboratory of Vanadium-Titanium Metallurgy and Advanced Materials, Chongqing University, Chongqing 400044, China; 17748351783@163.com (J.K.); 18883158379@163.com (Y.C.); zhongdapengcqu@163.com (D.Z.); lvxuewei@163.com (X.L.)

² College of Materials Science and Engineering, Chongqing University, Chongqing 400044, China

* Correspondence: qiuguibao@cqu.edu.cn

Abstract: Due to TiAl alloys' excellent properties, TiAl alloys have received widespread attention from researchers. However, the high energy consumption and lengthy process of traditional preparation methods have always limited the large-scale application of TiAl alloys. This article develops a new method for preparing TiAl-based alloy powder via the magnesium thermal reduction of TiO₂ in AlCl₃-KCl molten salt. In this study, the proportion of AlCl₃&KCl molten salts was determined. We conducted phase analysis on the final product by studying the changes in temperature and time. It was found that the TiAl₃ alloy powder could be obtained by being kept at 750 °C for 2 h, with an oxygen content of 3.91 wt%. The reaction process for the entire experiment was determined through thermodynamic calculations and experimental analysis, and the principles of the reduction process are discussed.

Keywords: TiAl alloy; magnesium reduction; AlCl₃-KCl; TiO₂



Citation: Kang, J.; Cui, Y.; Zhong, D.; Qiu, G.; Lv, X. A New Method for Preparing Titanium Aluminium Alloy Powder. *Metals* **2023**, *13*, 1436. <https://doi.org/10.3390/met13081436>

Academic Editor: Wislei Riuper Osório

Received: 5 July 2023

Revised: 2 August 2023

Accepted: 7 August 2023

Published: 10 August 2023



Copyright: © 2023 by the authors. Licensee MDPI, Basel, Switzerland. This article is an open access article distributed under the terms and conditions of the Creative Commons Attribution (CC BY) license (<https://creativecommons.org/licenses/by/4.0/>).

1. Introduction

Metal compounds offer both the plasticity of metals, and the high-temperature strength of ceramics in specific compositions, due to the metal compound ordered arrangement of their atoms, and the coexistence of inter-atomic metal bonds and covalent bonds. TiAl-based intermetallic compounds were highly valued in the aerospace industry and other fields, due to their excellent mechanical properties and low density, in the 1950s [1,2]. Nowadays, the TiAl-based alloy is still recognized as a high-end material in the world [3,4]. Due to its high specific strength, high temperature resistance [5,6], corrosion resistance, oxidation resistance [7,8], and excellent biocompatibility, the TiAl-based alloy is widely used in the field of high-end materials in modern life [9,10]. For example, large aeroplanes, submarines, aerospace technology, and artificial bones [11–13]. This high-end material should also be popularized in ordinary daily life but, due to its high cost, it has not been applied, and can only be applied in high- and middle-value fields. The reason for this dilemma is the long cycle and high cost of preparing the metal Ti. Since the discovery of metallic titanium, only the Kroll method has produced sponge titanium on a large scale [14–17]. Therefore, most methods for preparing TiAl-based alloys are element approaches [18–21], prepared by adding proportional amounts of the elements Ti and Al in a high-temperature melting furnace. Adding Ti separately also causes production costs for TiAl-based alloys.

Many researchers have adopted different methods to find an efficient method for producing TiAl-based alloys. The most traditional way is to prepare TiAl-based alloys via casting [22–25] and cast alloys with different compositions using a vacuum induction melting furnace, centrifuge, hot press, and other equipment. Among them, J Lapin [26] et al. prepared the Ti-42.6Al-8.7Nb-0.3Ta-2.0C and Ti-41.0Al-8.7Nb-0.3Ta-3.6C (in at.%) TiAl alloys via the casting method, and studied the effect of adding 2.0C and 3.6C on the properties of the TiAl alloys. They also studied the solid-state phase transformation grain refinement of the

as-cast peritectic TiAl-based alloys. Powder metallurgy is also the preparation method for most TiAl-based alloys; it can overcome the defects generated through traditional manufacturing methods, and obtain uniform and fine microstructures, significantly improving the mechanical properties of the alloys. Heike Gabrisch et al. [27] added 0.5–1.0 at.% C into Ti-45Al-5Nb alloy via powder metallurgy, and used a transmission electron microscope and high-energy XRD to study the influence of solid-solution carbon and carbide precipitation on the hardness of the TiAl alloy. In addition to the above two methods, emerging additive manufacturing technologies [28–30] can also prepare designed alloys, by stacking powders layer by layer. The powder preparation methods mentioned above all require titanium powder as a raw material, which is expensive, and increases production costs. Therefore, there is a need for a method that can directly prepare alloys from TiO_2 , to improve the existing technology, reduce the process flow, and increase the popularity of TiAl-based alloys [31,32].

Researchers have now prepared TiAl-based alloys using other methods. Zhao et al. [33,34] proposed a two-step thermal reduction method for preparing TiAl-based alloys. In this method, firstly, Na_2TiF_6 is reduced by TiAl-based alloy powder, which is the first reduction stage. After vacuum distillation, the second-stage reduction of Al is carried out, to obtain TiAl-based alloys. The TiAl-based alloy powder collected in the purification process can also be used for the first-stage reduction. This method successfully realizes the overall round-robin preparation of TiAl-based alloys through the Al thermal reduction of Na_2TiF_6 . Dou, Song, and Zhang [35,36] successfully prepared 20 kg TiAl-based alloy ingots with an oxygen content of approximately 1.09 wt% through multi-stage profound reduction. This method successfully achieved the one-step preparation of TiAl-based alloys through adding KClO_3 as a heating agent, and self-propagating aluminium heat.

However, the two-step aluminothermic reduction of Na_2TiF_6 , and the high-temperature self-propagation method, require experiments at high temperatures, resulting in energy consumption. However, due to the limited reduction effect of metal aluminium on TiO_2 at low temperatures, it is impossible to prepare TiAl-based alloys by reducing TiO_2 at low temperatures. Moreover, TiAl-based alloy ingots exhibit significant room temperature brittleness, with a derivation rate of less than 1%, and fracture during stretching, resulting in a poor machinability, and difficulties in their application. Due to the significant difference in melting points between Ti and Al, casting high-quality alloy ingots is difficult and costly. This article proposes a new method of preparing TiAl-based alloy powder by reducing TiO_2 in AlCl_3 & KCl molten salt through a magnesiothermic reduction. This method can only be carried out at low temperatures, with a simple production method, and a low level of environmental pollution. This work provides new ideas for the future large-scale application of TiAl-based alloy powder, and to solve the problem of the long preparation process of existing TiAl-based alloys.

2. Materials and Method

2.1. Materials

Anhydrous AlCl_3 , KCl , HCl , TiO_2 , and binder were obtained from Aladdin Reagent Co., Ltd. (Shanghai, China). The particle size of anhydrous AlCl_3 , KCl , and TiO_2 is below 74 μm . The binder used in this paper is ethyl cellulose, a polymer compound with the chemical formula $(\text{C}_{12}\text{H}_{22}\text{O}_5)_n$. Ethyl cellulose is a white powder at room temperature. The primary function of this binder is to aggregate the raw materials, and increase the contact area of raw materials. Under high-temperature conditions, ethyl cellulose will be decomposed into organic compounds that do not impact the experiment. As a reducing agent, Mg powder is obtained from Sinopharm Chemical Reagent Co., Ltd. (Ningbo, China). The Mg powder particle size is below 200 μm .

2.2. Introduction to AlCl_3 and Selection of AlCl_3 -KCl Molten Salt Ratio

AlCl_3 is a white crystalline powder with a solid hydrochloric acid odour, and a light yellow industrial product, and is easily soluble in water, alcohol, chloroform, etc. Its melting point is $194\text{ }^\circ\text{C}$, but it is prone to sublimation and deliquescence at $178\text{ }^\circ\text{C}$. Moreover, due to the exothermic hydration reaction, it may explode when encountering water. Therefore, the AlCl_3 must be sealed and stored in a dry environment.

(1) Physical properties of AlCl_3

AlCl_3 was first prepared by Biltz. W [37] in 1923, via the reaction of 99.5% pure Al powder with dry HCl gas. Subsequently, Baker Analytics and Grothe studied the basic properties of AlCl_3 , etc. [37]. The density and viscosity of AlCl_3 are key physical properties during the thermal reduction process. Based on previous research data, the density of AlCl_3 varies with the temperature, as shown in Figure 1. It can be seen that the density of AlCl_3 shows a steady downward trend with the temperature rising within $460\text{--}560\text{ }^\circ\text{C}$. The following formula is the density formula, fitted according to the data (estimated standard error: 0.15%).

$$\rho = 2.19 - 5.40 \times 10^{-4}T - 1.14 \times 10^{-5}T^2 + 3.04 \times 10^{-8}T^3 \quad (1)$$

ρ indicates the density of AlCl_3 ($\text{g}\cdot\text{cm}^{-3}$); T indicates the temperature ($^\circ\text{C}$).

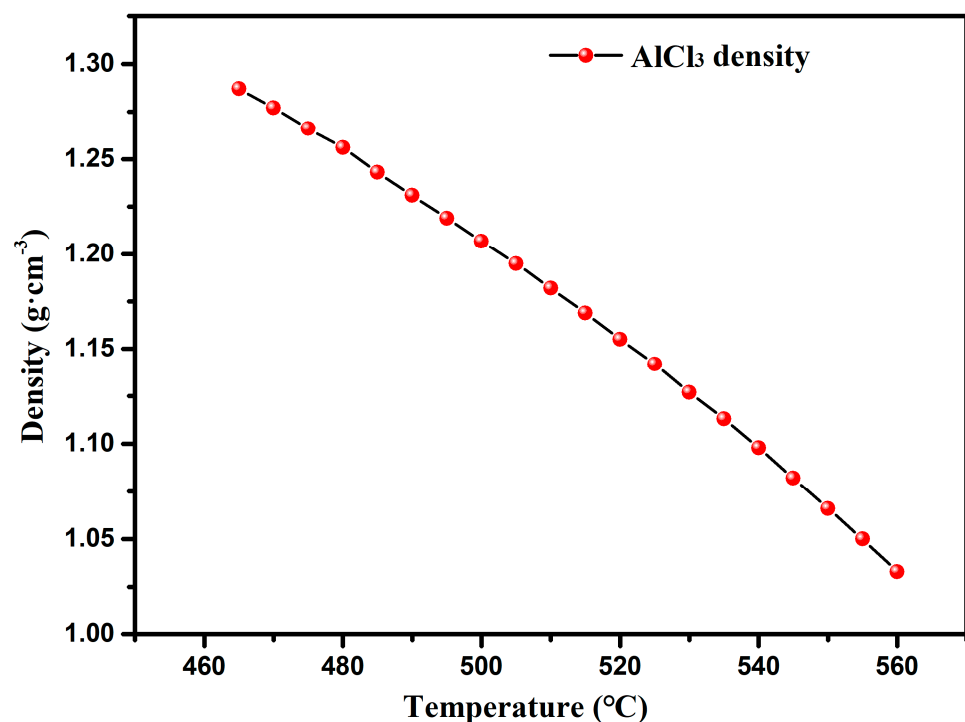


Figure 1. AlCl_3 density changes with temperature, data from [37].

Figure 2 shows the viscosity data of AlCl_3 . According to these data, the viscosity formula of AlCl_3 is fitted, and the estimated standard error is 1.05%.

$$\eta = 1.71 \cdot \exp(4943.8/RT) \quad (2)$$

η indicates the viscosity of AlCl_3 ($\text{Pa}\cdot\text{s}$), and R indicates a constant of 8.314 (kJ/mol); T indicates the temperature ($^\circ\text{C}$).

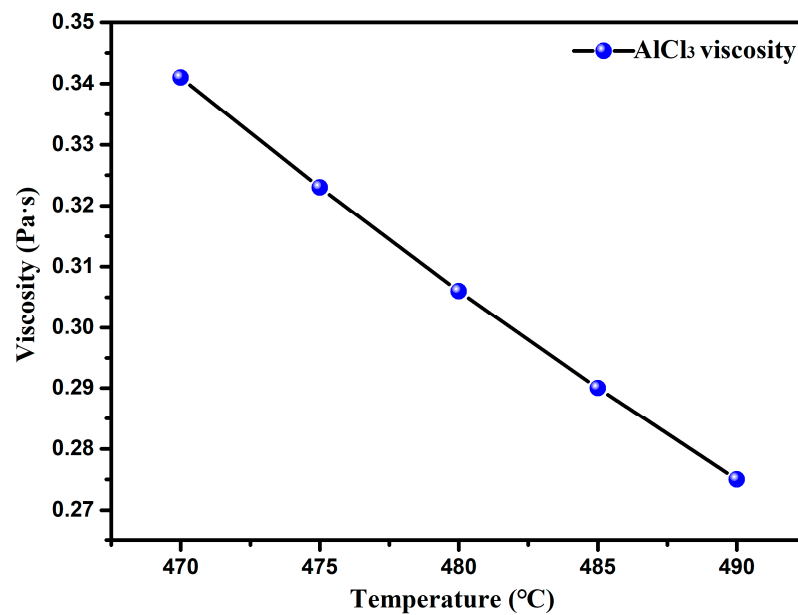


Figure 2. AlCl₃ viscosity changes with temperature, data from [37].

From the graph showing the viscosity and density changes with temperature, it can be seen that the density and viscosity of AlCl₃ show an overall decreasing trend with an increasing temperature. The decrease in density and viscosity is conducive to the complete contact of reactants during the reduction reaction process, increasing the reaction efficiency, which is a favourable factor in magnesium thermal reduction.

(2) Basic Physical Properties of AlCl₃-KCl Mixed Molten Salt

Due to the low melting point and easy sublimation of AlCl₃, to prevent the loss of raw materials due to the large amount of sublimation and volatilization of AlCl₃, a mixed molten salt AlCl₃-KCl is configured, which can effectively suppress the volatilization of AlCl₃. As shown in Figure 3, when the AlCl₃ content accounts for 80 wt% and above, the binary phase diagram of AlCl₃-KCl shows that a large amount of AlCl₃ gas is generated. As the KCl increases, the blue part in the figure shows the liquid phase zone of the AlCl₃-KCl eutectic salt without gas generation. Therefore, this part can be selected as the area used in the raw material ratio in this experiment, where the mass ratio of AlCl₃/(AlCl₃-KCl) is 0.65.

The density of the AlCl₃-KCl is based on Carter and Morrey's [37] work to obtain the following AlCl₃-KCl density data, as shown in Table 1. The temperature dependence of AlCl₃-KCl under different KCl contents was plotted using Table 1, as shown in Figure 4. It can be seen that as the KCl content increases, the overall density of the AlCl₃-KCl shows an upward trend. As the temperature increases, the density of the AlCl₃-KCl decreases. When the molar ratio of KCl exceeds 50%, the overall density of the AlCl₃-KCl does not change significantly with temperature. The incremented density is due to the melting point of KCl being higher. After the KCl content increases, the overall melting point of the AlCl₃-KCl increases. An increasing KCl content can inhibit AlCl₃ volatilization. This result is consistent with the calculation results in Figure 4.

Table 1. The density of the AlCl₃-KCl varies with the KCl content.

Mol % KCl	$\rho = a + bT$		Standard Error
	a	$b \cdot 10^{-3}$	
20.00	2.0252	−1.0038	0.11%
33.33	1.9889	−0.7901	0.14%
50.03	1.9556	−0.6622	0.05%
66.66	1.9734	−0.6101	0.02%

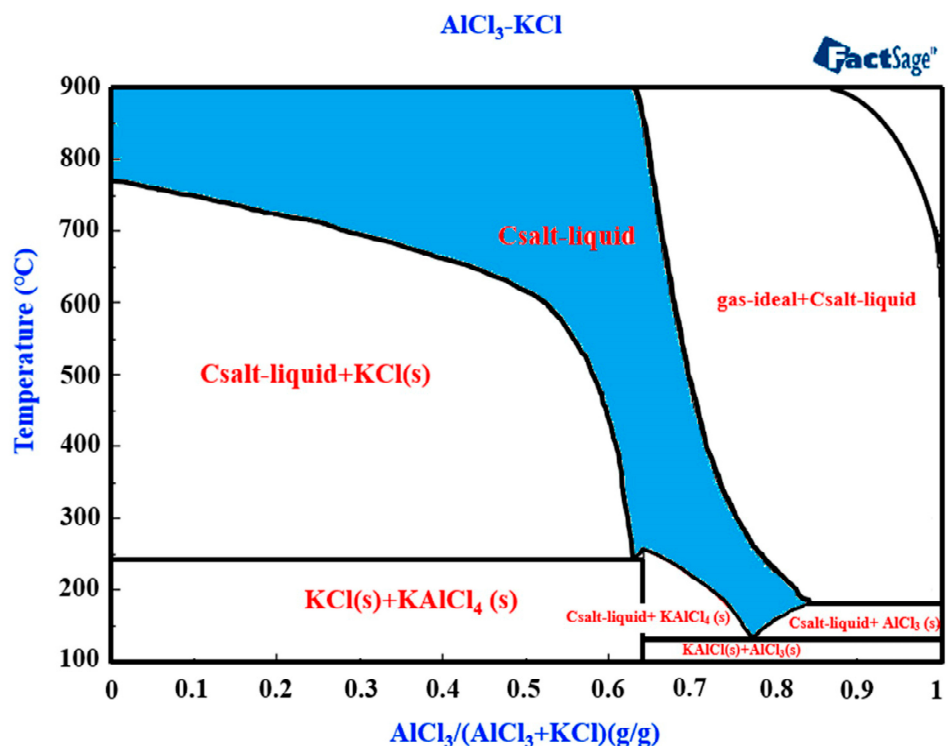


Figure 3. Binary phase diagram of AlCl₃-KCl.

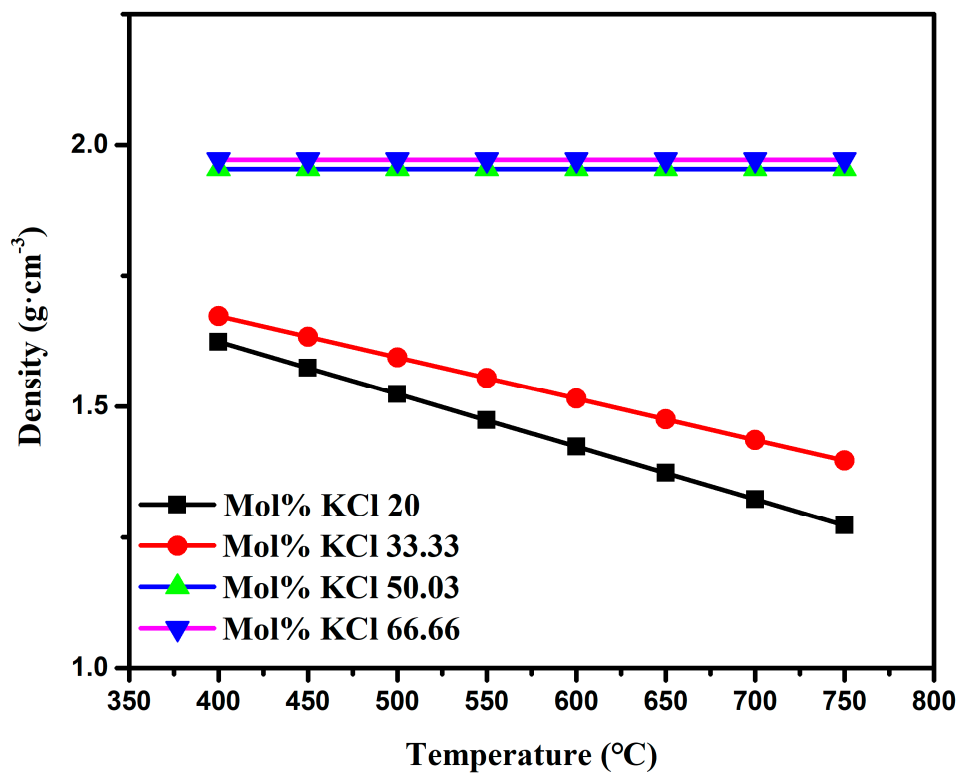


Figure 4. Density variation in AlCl₃-KCl with the temperature, under different KCl contents.

2.3. Methods

The raw materials are mixed with the binder in a mortar. After that, the mixed raw materials are pressed into a round green mass. For the reduction, we place the green mass into the molybdenum crucible and the tube furnace (KF1100 Nanjing Boyuntong (Nanjing, China), as shown in Figure 5). After reaching the specified temperature, this furnace can be loaded into the reaction furnace tube. The heating rate is 15 °C/min, and the insulation is maintained after reaching the specified temperature. According to the analysis of the physical properties and phase diagram of AlCl₃&KCl in the previous section, to suppress the volatilization of AlCl₃, the molten salt is weighed based on the mass ratio of AlCl₃/(AlCl₃+KCl) of 0.65. Therefore, this experiment's molten salt mass ratio of AlCl₃:KCl is 1.8. Considering that AlCl₃ has the characteristic of volatilizing at low temperatures, it is necessary to increase the content of AlCl₃ appropriately during the raw material configuration process. The amount of TiO₂ used in each experiment is 5 g, the proportion of molten salt is four times the total mass of the TiO₂ added, and the amount of magnesium added is the molar mass of the AlCl₃ completely reacted.

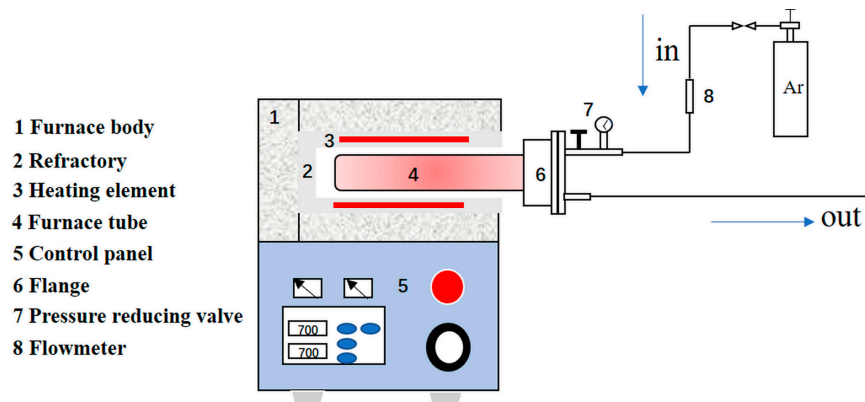


Figure 5. Experimental device.

The experimental process is shown in Figure 6. The experiment was conducted in a tubular box mixing furnace. The raw materials were mixed evenly, loaded into a molybdenum crucible, and placed in a reactor. Inert gas was first introduced into the reactor to exhaust the air, with a flow rate of 300 mL/min. After the high-temperature furnace rose to the set temperature, the reactor was loaded into the furnace, without increasing the temperature of the furnace (to reduce the evaporation of the molten salt). This experiment explored the influence of time on the reaction products' phase and oxygen content. The overall reaction time starts from the installation of the reaction furnace tube into the furnace, and a specific insulation time is set. After the reaction, argon gas is continuously introduced and cooled in the furnace, to ensure that the sample does not come into contact with oxygen. The final reactant is extracted for subsequent acid leaching and flotation, to obtain the final alloy product for analysis. Among the experiments, 5 wt% dilute HCl is used for acid leaching. The acid-leaching process is carried out in a water bath at 80 °C for 2 h. The acid-leaching process is mainly used to remove Mg and MgO. The specific reactions are shown in the formulae below. The reaction byproduct Al₂O₃ is removed via ball milling. The mass ratio of the ball-milling process as ball:material:H₂O during ball milling is 1.6:1:3. The ball mill rotates at a speed of 350 r/min for 15 min each time. Each experiment requires ball milling at least three times.



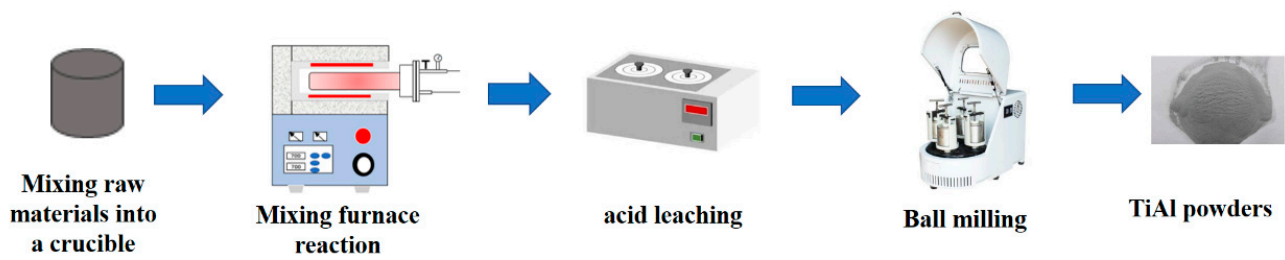


Figure 6. Experimental flowchart.

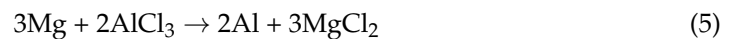
2.4. Analysis

X-ray powder diffraction (XRD, Cu K α radiation, PANalytical X'Pert Powder, Malvern PANalytical B.V., Almelo, The Netherlands), with a scanning range of 10–90° and a scanning step of 5 deg./min, was carried out, to confirm the phase composition of sample powder three times. Scanning electron microscopy (SEM, TESCAN VEGA 3 LMH system, TESCAN, Brno, Czech Republic) was also performed, to evaluate the microanalysis and surface morphology of the reaction product. Energy-dispersive spectroscopy (EDS) microanalysis was conducted. The accelerating voltage used for the EDS analysis was 10 kV. The thermodynamic software FactSage8.0 calculated the feasibility of the reaction. The oxygen content of the product was analyzed using the JXA82 electron probe from JEOL Corporation, and the particle size analyzer from NanoBrook Omni of Brookhaven Instruments, Holtsville, NY, USA.

3. Results and Discussion

3.1. Phase Analysis of Reactants at Different Temperatures

The XRD phase diagrams and SEM of the products at different reaction temperatures are shown in Figures 7 and 8. Comparing the XRD analyses of the products at reaction temperatures of 750–950 °C, it can be found that the reaction products are TiAl-based alloy powders. Compared with traditional magnesiothermic reduction, TiO₂ is not directly reduced; other substances participate in the reaction. The Gibbs free energy diagram of the reaction between Mg and AlCl₃, TiO₂, was drawn using the thermodynamic software FactSage8.0, as shown in Figure 9. At temperatures ranging from 400 °C to 950 °C, the Gibbs free energy of the reaction between Mg and AlCl₃, TiO₂ can be observed. At the same magnesium content, Mg preferentially reacts with AlCl₃, and the entire process uses aluminium as a reducing agent in reducing the TiO₂. Moreover, magnesium-reducing AlCl₃ releases a large amount of heat, to drive the aluminothermic reduction of TiO₂. Therefore, the entire reaction process is as follows:



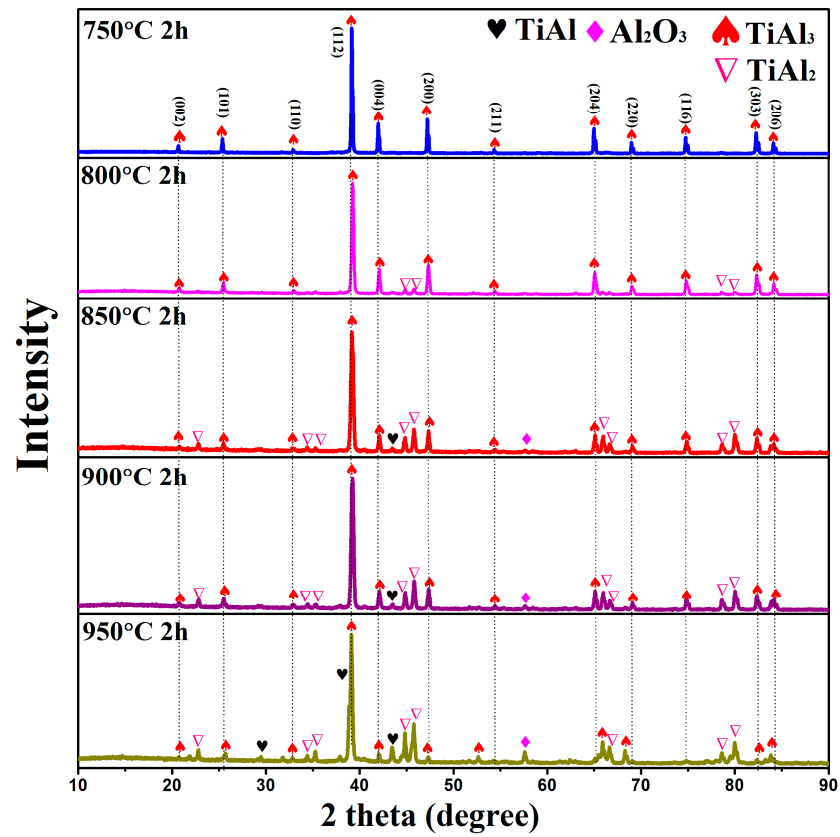


Figure 7. XRD patterns of products at different temperatures.

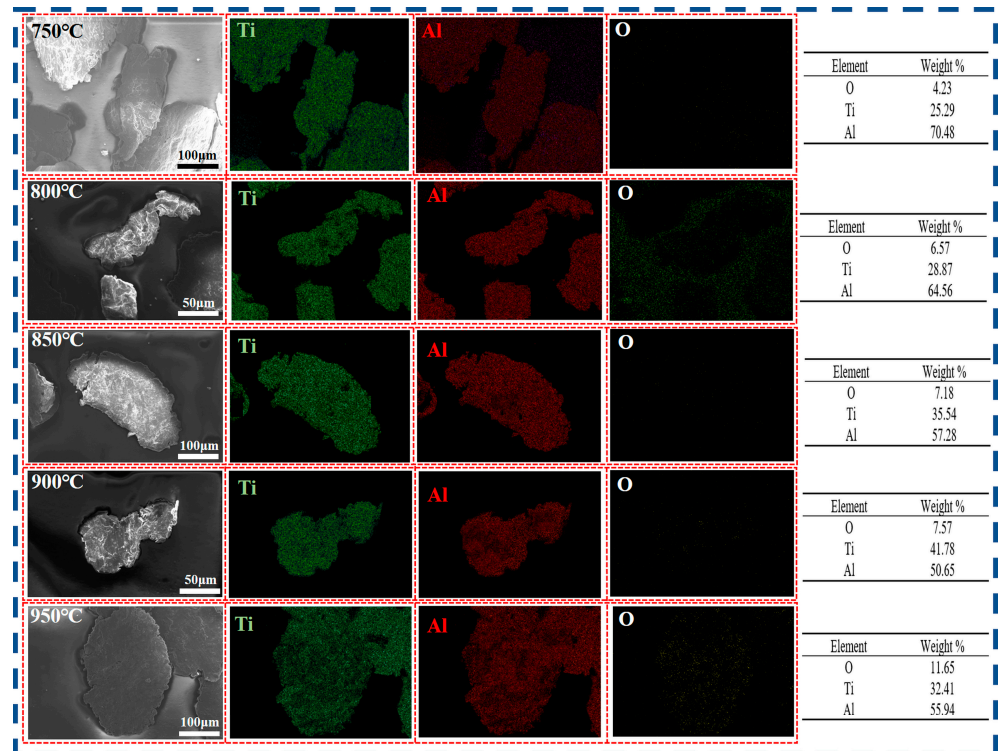


Figure 8. SEM and surface scanning of magnesium thermal reduction products, assisted by the AlCl₃&KCl molten salt medium.

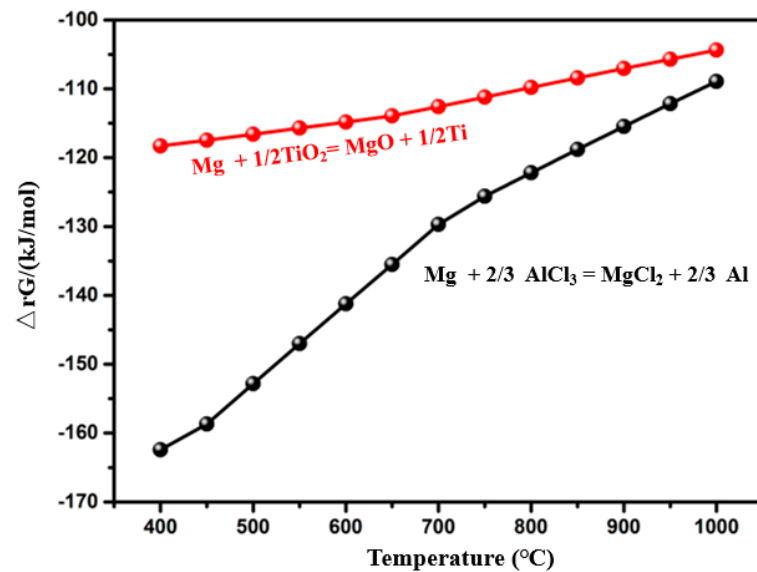


Figure 9. Gibbs free energy of the reaction between AlCl_3 and TiO_2 , with Mg.

According to literature reports [38], the alloy reaction between Al and Ti at low temperatures is mainly liquid–solid. In this experiment, the main product phase is the TiAl_3 alloy after 2 h of reaction at 750 °C. As the reaction temperature increases, from 800 °C to 950 °C, the peak of TiAl_3 gradually decreases, while the peak of TiAl_2 gradually increases. The peak of TiAl_2 gradually increases because external Al reacts before Ti to generate TiAl_3 during the reaction process, and then gradually forms TiAl_2 , as shown in Equation (8). The increase in temperature is more conducive to the formation of the TiAl alloy. From the energy spectrum detected via SEM surface scanning, it can be seen that the obtained TiAl alloy has a uniform distribution of components, with an oxygen content of 4.23 wt%. The reason for such a high oxygen content is that the reduction effect of Al is limited, and TiO_2 cannot be reduced to a lower oxygen content state. However, due to the presence of Mg, some O is absorbed, to some extent. As the reaction temperature increases, it is found that the oxygen content in the reaction product is low, at 750 °C.

3.2. Effect of Reduction Temperature

In the previous section, the study of different reaction temperatures in the magnesiothermic reduction of TiO_2 in the AlCl_3 & KCl molten salt system found that the oxygen content of the TiAl_3 -based alloys generated at 750 °C was relatively low and stable. Therefore, 750 °C was chosen as the optimal reaction temperature. This section takes the reaction time as a single variable, and experimentally studies the effect of different reaction times on the preparation of TiAl-based alloys at 750 °C. We set the reaction time at 750 °C for 1, 2, and 4 h, respectively, to study the effect of the reaction time on the reduction effect during the reaction process. Figures 10 and 11 show that XRD and SEM characterized the reaction products. After reacting at 750 °C for 1 h, the main phases of the reaction products are TiAl_3 and metallic Al. The TiAl_3 alloy is caused by the short reaction time between Al and Ti, and some of the reduced Al has not yet formed an alloy with Ti. Therefore, a large amount of metal Al has not reacted in the product after one hour of reaction. With the extension of the reaction time, when the reaction temperature is 2 h, the main product of the reaction is TiAl_3 . After further prolonging the reaction time to 4 h, the main reaction products are the TiAl alloy, and a small amount of Al_2O_3 . The occurrence of Al_2O_3 is because, with the extension of the reaction time, some Al forms Al_2O_3 powder through solid-state diffusion with the alloy, after reducing the TiO_2 . This Al_2O_3 cannot be removed from the surface of the alloy through acid leaching and flotation. The attached Al_2O_3 can be seen in the SEM image in Figure 12; a small amount of matte and rough surface substance is attached to the metal surface, which is the Al_2O_3 generated through the extended reaction time.

As mentioned above, a stable $TiAl_3$ alloy powder can be obtained by reacting TiO_2 with $AlCl_3$ & KCl molten magnesium salt for 2 h at $750\text{ }^\circ\text{C}$.

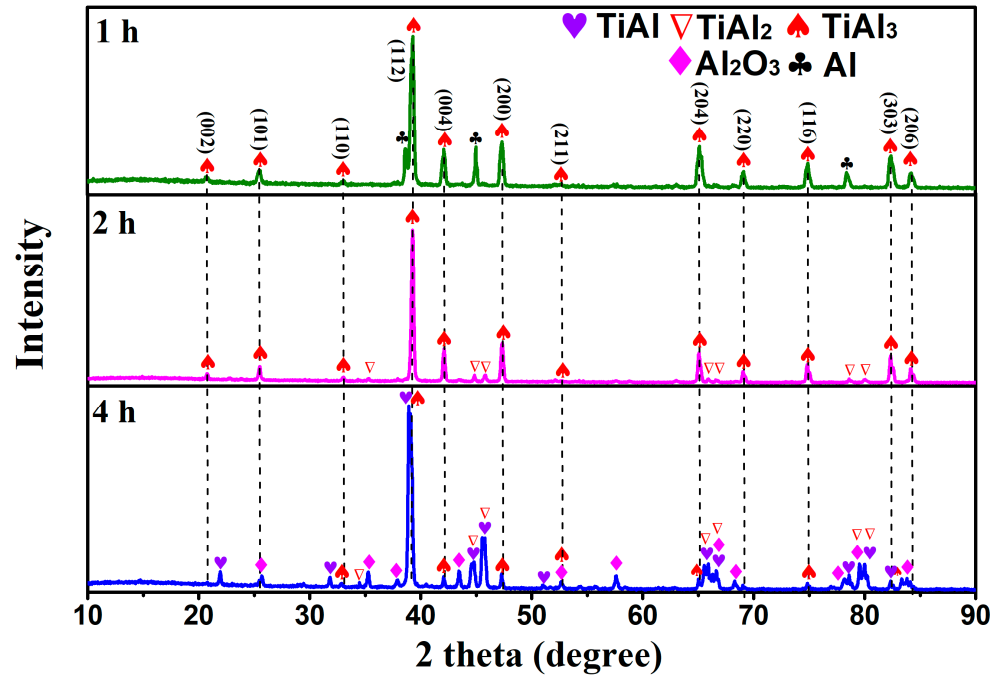


Figure 10. Effect of different reduction times on the reduction products.

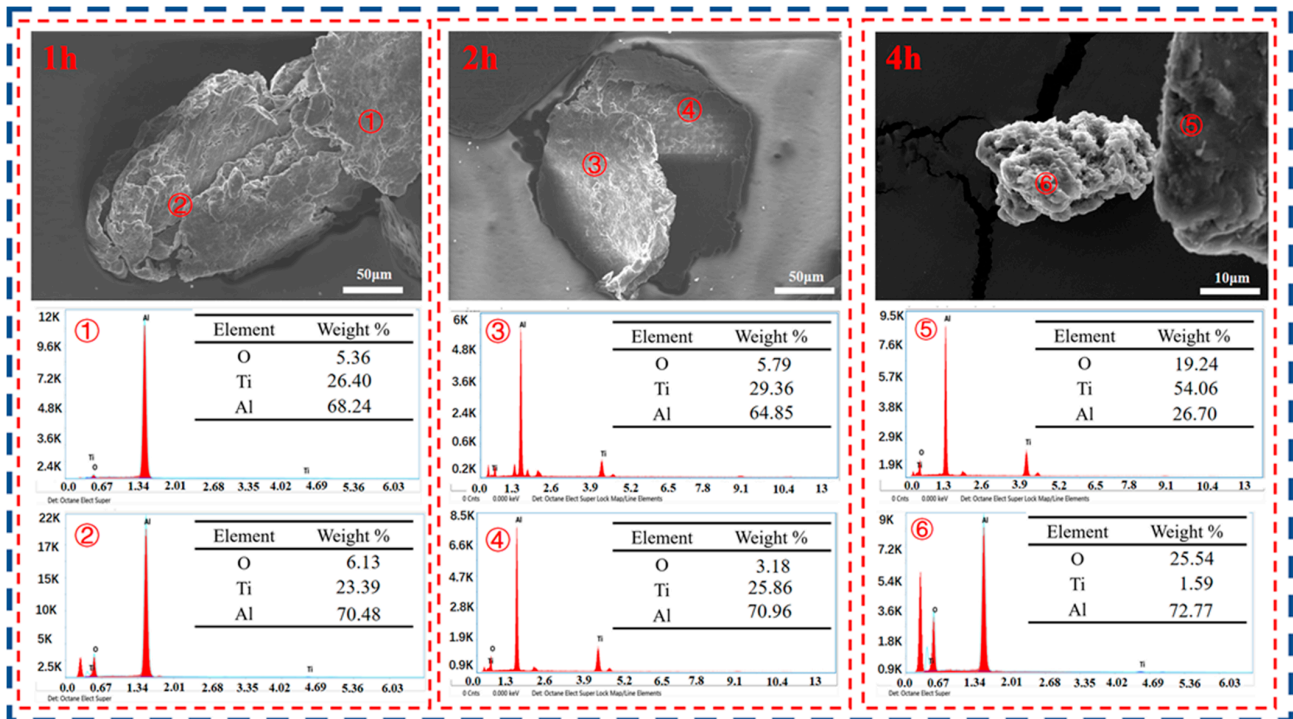


Figure 11. SEM and EDS of products with different reduction times.

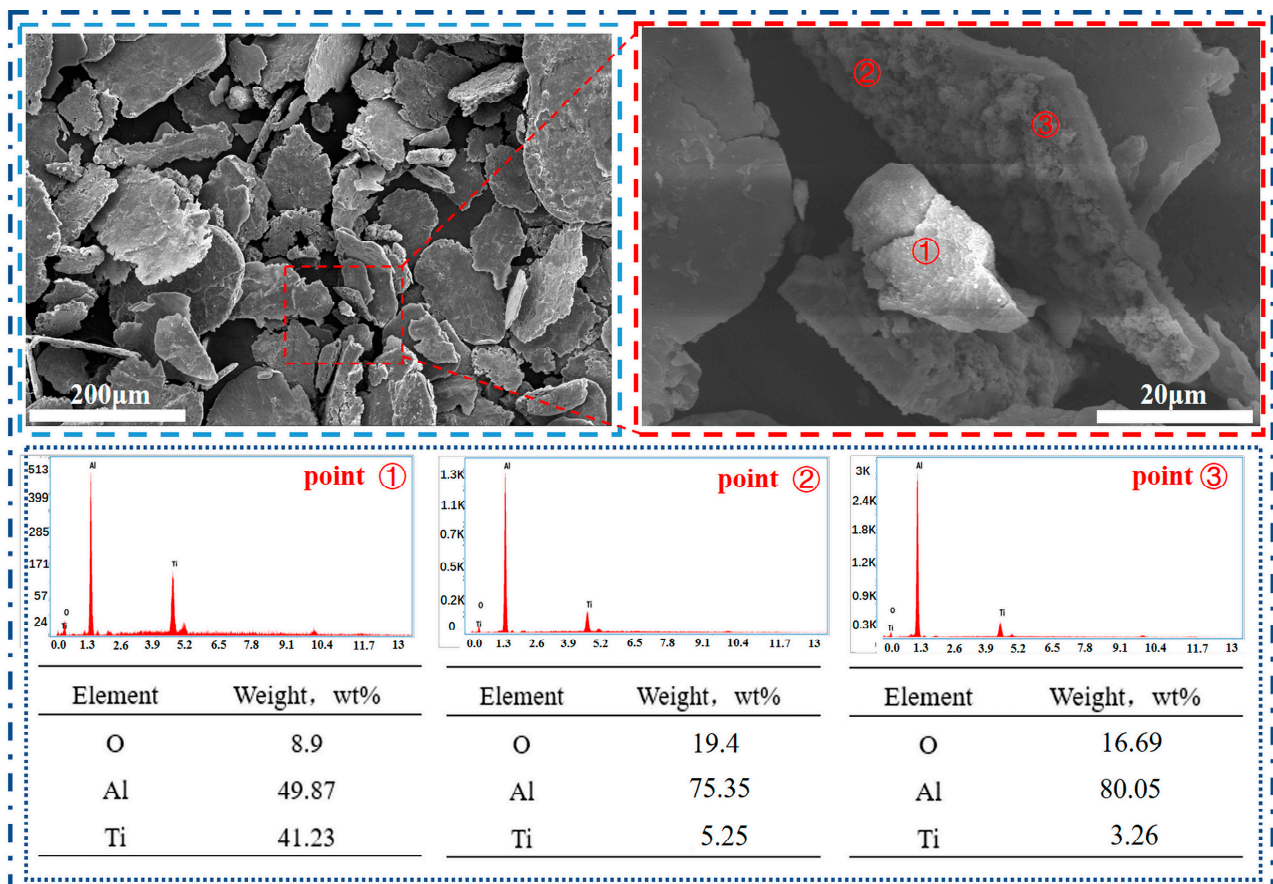


Figure 12. Scanning electron microscopy (SEM) images and energy-dispersive spectroscopy (EDS) of the products at 950 °C.

As the reaction time increases, the oxygen content in the reaction product gradually increases. At the same time, this is also because the solid-phase-to-solid-phase diffusion reaction between the Al_2O_3 and TiAl-based alloys occurs at high temperatures, which finally causes part of the Al_2O_3 to enter the TiAl alloy phase, as shown in Figure 12. The TiAl alloy powder is a coarse powder bonded to the surface of the TiAl alloy, with a high oxygen content and no Ti element, which can be determined as Al_2O_3 powder. Based on the above analysis, the optimal reaction temperature for the thermal reduction of AlCl_3 & KCl mixed molten salt magnesium is 750 °C, and the main product generated by the reaction at 750 °C is TiAl_3 . The oxygen content of the product was analyzed using the JXA82 electric probe. The effect of the reaction time on the oxygen content of the product is shown in Figure 13, with the lowest oxygen content of 3.91 wt% after two hours of reaction.

3.3. Analysis of the AlCl_3 & KCl -Molten-Salt-Assisted Magnesium Thermal Reduction Process

The above experiments indicate that the AlCl_3 & KCl molten salt system serves as a medium for the magnesium thermal reduction of TiO_2 , to prepare TiAl_3 alloy powder. The schematic diagram of the entire reaction process is shown in Figure 14. At the beginning of the reaction, Mg is ionized in the molten salt to form Mg^{2+} , which reacts with Cl^- in the molten salt to form MgCl_2 , while Al^{3+} is reduced to metallic aluminium. At this time, the metallic aluminium is not covered by a surface oxide film, and the generated liquid metal Al reacts with TiO_2 to generate TiAl-based alloys. The melting temperature of Al is relatively low. At 750 °C, a liquid–solid reaction occurs between the Al liquid and the reduced Ti solid, generating TiAl_3 on the surface of the titanium. Afterwards, the internal metal Ti reacts with TiAl_3 to generate TiAl_2 . With the prolongation of the holding time, various TiAl-based alloys react, to generate TiAl alloy powder. The entire TiAl alloy

formation process is shown in Equations (5)–(9). This experiment can prepare TiAl_3 alloy powder stably at $750\text{ }^\circ\text{C}$ for 2 h, demonstrating a new method for preparing TiAl alloy at low temperatures. Moreover, the TiAl_3 alloy powder has a low density, high modulus, and strong oxidation resistance, making it an excellent high-temperature structural and layer material.

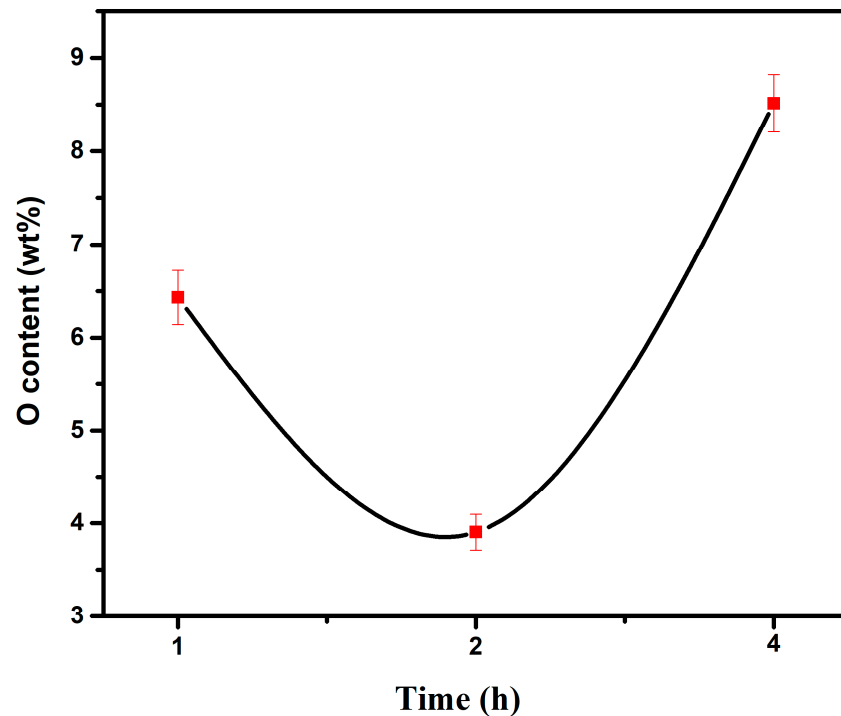


Figure 13. The effect of different reaction times on the oxygen content of products.

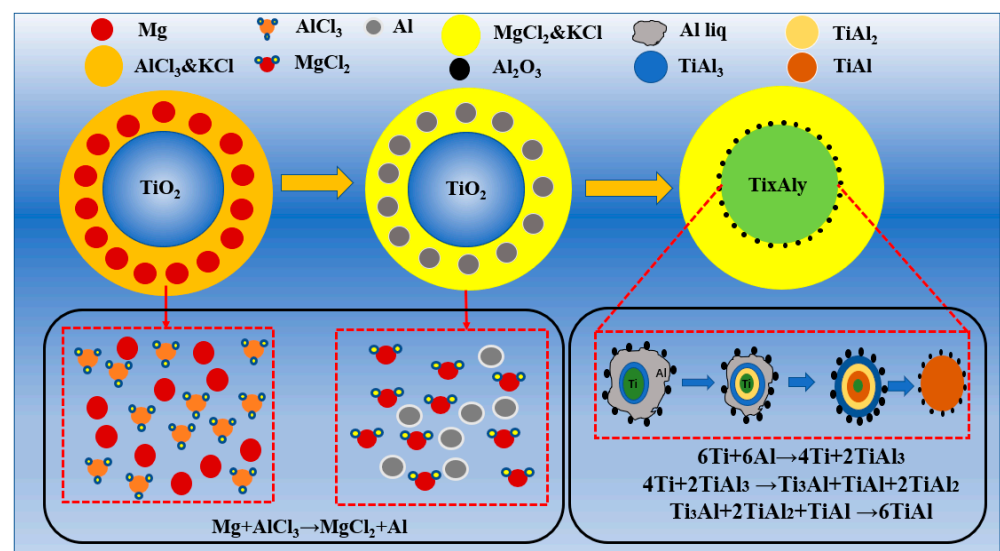


Figure 14. Schematic diagram of the AlCl_3 & KCl -molten-salt-assisted magnesium thermal reduction process.

3.4. Product Analysis and Comparison

The elements of the TiAl_3 alloy powder product prepared in this experiment are shown in Table 2, and the particle size is shown in Figure 15. The Ti content is approximately 28.41 wt%, and the Al content is approximately 67.68 wt%. The TiAl_3 alloy prepared in this experiment has a larger particle size. The final products D10, D50, and D90 were

135 μm , 453 μm , and 912 μm , respectively. From the discovery of metallic titanium to the current preparation of titanium alloys, in addition to traditional high-temperature melting and mechanical alloying, many low-cost methods have also been used for preparing TiAl-based alloys. The TiAl-based alloy shows an excellent performance. Developing low-cost and straightforward equipment for new processes, to meet increasing performance requirements, is a hot research topic. These new processes all have the advantages of continuity and low cost. Among emerging technologies, high-temperature self-propagation is the most representative method, but the process controllability of this method is too poor, and there are certain risks. The multi-level deep reduction method is also a relatively novel method that has recently emerged. Still, it also has the problem of a high reaction temperature, which leads to a high energy consumption. Table 3 compares new methods for preparing TiAl-based alloys in recent years, and this experiment. These preparation processes for preparing metallic titanium alloys are currently at the laboratory stage, and there is still a long way to go from the laboratory to industrial production.

Table 2. Composition of the TiAl₃ alloy (wt%).

Ti	Al	O
28.41	67.68	3.91

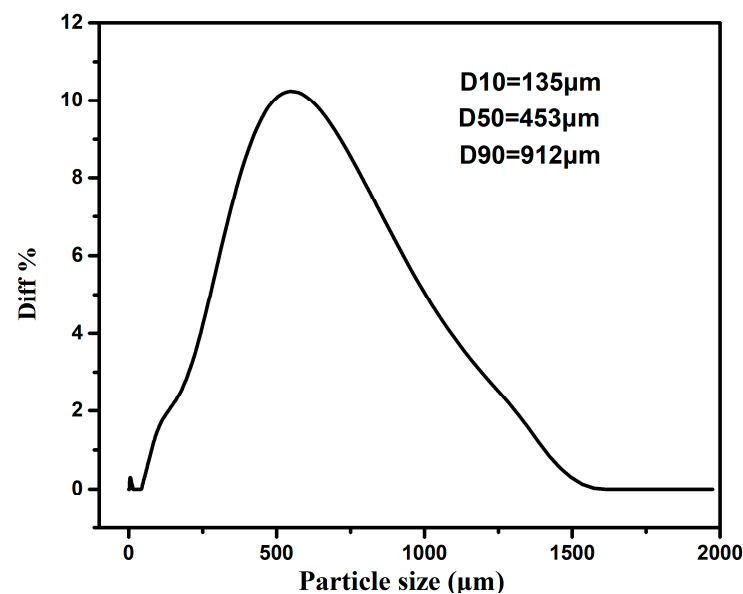


Figure 15. Particle size distribution of the TiAl₃ alloy powder.

Table 3. Comparison of new methods for titanium alloy preparation.

Method	Features	Advantages	Disadvantages
Perform reduction process (PRP) [39]	Ca as a reducing agent	Complete reaction with a high recovery rate	Unable to apply on a large scale
SHS process [40]	Spontaneous reaction through the heating agent	Efficiency, high energy consumption, and low consumption	Uncontrollable reaction process
Two-stage thermite process [41]	Reduction using Na ₂ TiF ₆ as a raw material	Short process and low energy consumption	Multiple reactions
AlCl ₃ &KCl-molten-salt assisted magnesium thermal reduction	Low temperature, AlCl ₃ &KCl as the reaction medium	Low energy consumption, controllable reaction	AlCl ₃ volatilization

4. Conclusions

This article proposes a new process for preparing TiAl₃ alloy powder, mainly discussing how AlCl₃&KCl molten salt can prepare TiAl₃ alloy powder via the magnesium thermal reduction of TiO₂. At the same time, the influence of different experimental factors on the reduction effect is studied, mainly the influence of the reduction temperature and time on the product phase and oxygen content. Based on the experimental research, the following main conclusions have been drawn:

- (1) Through the study of the basic physical properties of the AlCl₃ and AlCl₃&KCl, it was found that the density of the AlCl₃ decreased from 1.3 g·cm⁻³ to 1 g·cm⁻³ in the temperature range of 460–560 °C, and the viscosity also decreased from 0.34 Pa·s to 0.27 Pa·s with the temperature. For AlCl₃&KCl eutectic salts, when the KCl content is 20 wt% and 33.33 wt%, the density of the AlCl₃&KCl decreases from 1.65 g·cm⁻³ to below 1.5 g·cm⁻³ within the range of 350–850 °C. However, when the KCl content is 50 wt% and 66.66 wt%, the temperature has little effect on the density change of the AlCl₃&KCl, with a density of approximately 2 g·cm⁻³. To reduce the volatilization of the AlCl₃, the experiment selected a mass ratio of 0.65 for the AlCl₃/(AlCl₃+KCl) as the selected eutectic salt ratio.
- (2) Using TiO₂ as the raw material, magnesium thermal reduction experiments were conducted in a AlCl₃&KCl molten salt medium, to clarify the reaction action and sequence of AlCl₃ during the reaction process. During the magnesium thermal reduction process, Mg preferentially reacts with AlCl₃ at 400–1000 °C to generate metal Al, which reacts with TiO₂, and generates TiAl₃ alloy powder at 750–950 °C.
- (3) When the experimental temperature is within the range of 750–950 °C, the products of the AlCl₃&KCl molten-salt-assisted magnesium thermal reduction gradually form a TiAl alloy from the TiAl₃ alloy at 750 °C to 950 °C. The oxygen content also increases from 4.23 wt% at 750 °C, to 11.23 wt% at 950 °C, and the final powder oxygen content also increases with the extension of the reduction time. After 4 h of reaction at 750 °C, the oxygen content reaches approximately 8.5 wt%, and the reaction temperature is at 950 °C; after 4 h of reaction time, it will cause an increase in, and adhesion of, the Al₂O₃ in the product. The optimal reaction time for this process is 2 h, and the reaction temperature is 750 °C. TiAl₃ alloy powders with Ti, Al, and O contents of 28.41 wt%, 67.68 wt%, and 3.91 wt% can be obtained, respectively. The powder particle size is concentrated at around 450 μm.

Author Contributions: Software, Y.C.; writing—original draft, J.K.; writing—review and editing, D.Z.; project administration, G.Q. and X.L. All authors have read and agreed to the published version of the manuscript.

Funding: This research was funded by National Natural Science Foundation of China, grant number [52074052].

Data Availability Statement: Not applicable.

Acknowledgments: The authors are incredibly grateful for a grant from the National Natural Science Foundation of China (Grant No.52074052).

Conflicts of Interest: The authors declare no conflict of interest.

References

1. Tetsui, T. Impact Resistance of Commercially Applied TiAl Alloys and Simple-Composition TiAl Alloys at Various Temperatures. *Metals* **2022**, *12*, 2003.
2. Wang, J.H.; Lu, Y.; Shao, X.H. First-Principles Calculation for the Influence of C and O on the Mechanical Properties of gamma-TiAl Alloy at High Temperature. *Metals* **2019**, *9*, 262.
3. Yang, Y.; Liang, Y.F.; Li, C.; Lin, J. Microstructure and Mechanical Properties of TiAl Matrix Composites Reinforced by Carbides. *Metals* **2022**, *12*, 790.
4. Mogale, N.F.; Matizamhuka, W.R. Spark Plasma Sintering of Titanium Aluminides: A Progress Review on Processing, Structure-Property Relations, Alloy Development and Challenges. *Metals* **2020**, *10*, 1080.

5. Wang, Z.H.; Sun, H.X.; Du, Y.L.; Yuan, J. Effects of Powder Preparation and Sintering Temperature on Properties of Spark Plasma Sintered Ti-48Al-2Cr-8Nb Alloy. *Metals* **2019**, *9*, 861.
6. Dong, Z.C.; Feng, A.H.; Wang, H.; Qu, S.; Wang, H. Thermodynamic Study on Initial Oxidation Behavior of TiAl-Nb Alloys at High Temperature. *Metals* **2023**, *13*, 485.
7. Zhu, X.P.; Zhu, C.L.; Lin, B.S.; Wang, Z. Research on Optimization Design of Cast Process for TiAl Case Casting. *Metals* **2022**, *12*, 1954.
8. Williams, J.C.; Boyer, R.R. Opportunities and Issues in the Application of Titanium Alloys for Aerospace Components. *Metals* **2020**, *10*, 705.
9. Zhang, S.L.; Cui, N.; Sun, W.; Li, Q. Microstructural Characterization and Crack Propagation Behavior of a Novel beta-Solidifying TiAl Alloy. *Metals* **2021**, *11*, 1231.
10. Yu, W.; Zhou, J.X.; Yin, Y.; Feng, X.; Nan, H.; Lin, J.; Ding, X.; Duan, W. Effects of Hot Isostatic Pressing and Heat Treatment on the Microstructure and Mechanical Properties of Cast TiAl Alloy. *Metals* **2021**, *11*, 1156.
11. Bewlay, B.P.; Nag, S.; Suzuki, A.; Weimer, M.J. TiAl alloys in commercial aircraft engines. *Mater. High Temp.* **2016**, *33*, 549–559.
12. Galati, M.; Gatto, M.L.; Bloise, N.; Fassina, L.; Saboori, A.; Visai, L.; Mengucci, P.; Iuliano, L. Electron Beam Powder Bed Fusion of Ti-48Al-2Cr-2Nb Open Porous Scaffold for Biomedical Applications: Process Parameters, Adhesion, and Proliferation of NIH-3T3 Cells. *3D Print. Addit. Manuf.* **2022**. [[CrossRef](#)]
13. Xu, R.; Li, M.; Zhao, Y. A review of microstructure control and mechanical performance optimization of γ -TiAl alloys. *J. Alloys Compd.* **2023**, *932*, 167611.
14. Subramanyam, R.B. Some recent innovations in the Kroll process of titanium sponge production. *Bull. Mater. Sci.* **1993**, *16*, 433–451.
15. Wang, W.; Wu, F. Quantifying Heat Transfer Characteristics of the Kroll Reactor in Titanium Sponge Production. *Front. Energy Res.* **2021**, *9*, 759781.
16. Wartman, F.S.; Baker, D.H.; Nettle, J.R.; Homme, V.E. Some Observations on the Kroll Process for Titanium. *J. Electrochem. Soc.* **1954**, *101*, 507–513.
17. Zhang, W.; Zhu, Z.; Cheng, C.Y. A literature review of titanium metallurgical processes. *Hydrometallurgy* **2011**, *108*, 177–188.
18. Kumaran, S.; Chantiah, B.; Rao, T.S. Effect of niobium and aluminium additions in TiAl prealloyed powders during high-energy ball milling. *Mater. Chem. Phys.* **2008**, *108*, 97–101.
19. Rao, K.P.; Du, Y.J. In situ formation of titanium silicides-reinforced TiAl-based composites. *Mater. Sci. Eng. A* **2000**, *277*, 46–56.
20. Wang, G.X.; Mao, X. Preparation of TiAl/Mo and TiAl/NiAl composites by powder processing. *J. Mater. Sci.* **1997**, *32*, 6325–6329.
21. Yan, M.; Yang, F.; Zhang, H.; Zhang, C.; Zhang, H.; Chen, C.; Guo, Z. Multiple intermetallic compounds reinforced Ti-48Al alloy with simple composition and high strength. *Mater. Sci. Eng. A* **2022**, *858*, 144152.
22. Pilone, D.; Pulci, G.; Paglia, L.; Mondal, A.; Marra, F.; Felli, F.; Brotzu, A. Mechanical Behaviour of an Al₂O₃ Dispersion Strengthened γ TiAl Alloy Produced by Centrifugal Casting. *Metals* **2020**, *10*, 1457.
23. Shen, Y.; Jia, Q.; Zhang, X.; Liu, R.; Wang, Y.; Cui, Y.; Yang, R. Tensile Behavior of SiC Fiber-Reinforced γ -TiAl Composites Prepared by Suction Casting. *Acta Metall. Sin.* **2021**, *34*, 932–942.
24. Tetsui, T. Selection of Additive Elements Focusing on Impact Resistance in Practical TiAl Cast Alloys. *Metals* **2022**, *12*, 544.
25. Yu, Y.; Kou, H.; Wang, Y.; Wang, Y.; Jia, M.; Li, H.; Li, Y.; Wang, J.; Li, J. Controlling lamellar orientation of Ti-47.5Al-5Nb-2.5V-1Cr alloy by conventional casting. *Scr. Mater.* **2023**, *223*, 115080.
26. Lapin, J.; Kamyshnykova, K.; Klimova, A. Comparative Study of Microstructure and Mechanical Properties of Two TiAl-Based Alloys Reinforced with Carbide Particles. *Molecules* **2020**, *25*, 3423.
27. Gabrisch, H.; Stark, A.; Schimansky, F.-P.; Wang, L.; Schell, N.; Lorenz, U.; Pyczak, F. Investigation of carbides in Ti-45Al-5Nb-xC alloys ($0 \leq x \leq 1$) by transmission electron microscopy and high energy-XRD. *Intermetallics* **2013**, *33*, 44–53.
28. Emiralioglu, A.; Ünal, R. Additive manufacturing of gamma titanium aluminide alloys: A review. *J. Mater. Sci.* **2022**, *57*, 4441–4466.
29. Liu, J.; Wang, M.; Zhang, P.; Chen, Y.; Wang, S.; Wu, T.; Xie, M.; Wang, L.; Wang, K. Texture refinement and mechanical improvement in beam oscillation superimposed laser welding of TiAl-based alloy. *Mater. Charact.* **2022**, *188*, 111892.
30. Liu, Z.-Q.; Zhu, X.-O.; Yin, G.-L.; Zhou, Q. Direct bonding of bimetallic structure from Ti₆Al₄V to Ti₄₈Al₂Cr₂Nb alloy by laser additive manufacturing. *Mater. Sci. Technol.* **2022**, *38*, 39–44.
31. Soliman, H.A.; Elbestawi, M. Titanium aluminides processing by additive manufacturing—A review. *Int. J. Adv. Manuf. Technol.* **2022**, *119*, 5583–5614.
32. Zhou, W.; Shen, C.; Hua, X.; Wang, L.; Zhang, Y.; Li, F.; Xin, J.; Ding, Y. The effect of vanadium on the microstructure and mechanical properties of TiAl alloy fabricated by twin-wire directed energy deposition-arc. *Addit. Manuf.* **2023**, *62*, 103382.
33. Zhao, K.; Feng, N.; Wang, Y. Fabrication of Ti-Al intermetallics by a two-stage aluminothermic reduction process using Na₂TiF₆. *Intermetallics* **2017**, *85*, 156–162.
34. Zhao, K.; Wang, Y.W.; Peng, J.P. Electrochemical preparation of titanium and titanium-copper alloys with K₂Ti₆O₁₃ in KF-KCl melts. *Rare Met.* **2017**, *36*, 527–532.
35. Song, Y.; Dou, Z.; Zhang, T.-A. Mechanisms of metal-slag separation behavior in thermite reduction for preparation of TiAl alloy. *J. Mater. Eng. Perform.* **2021**, *30*, 9315–9325.
36. Song, Y.; Dou, Z.; Liu, Y.; Zhang, T.-A. Study on the Preparation Process of TiAl Alloy by Self-Propagating Metallurgy. *J. Mater. Eng. Perform.* **2023**. [[CrossRef](#)]

37. Janz, G.J.; Tomkins, R.P.T.; Allen, C.B.; Downey, J.R.; Garner, G.L.; Krebs, U.; Singer, S.K. Molten salts: Volume 4, part 2, chlorides and mixtures—Electrical conductance, density, viscosity, and surface tension data. *J. Phys. Chem. Ref. Data* **1975**, *4*, 871–1178.
38. Školáková, A.; Leitner, J.; Salvetr, P.; Novák, P.; Deduytsche, D.; Kopeček, J.; Detavernier, C.; Vojtěch, D. Kinetic and thermodynamic description of intermediary phase formation in Ti-Al system during reactive sintering. *Mater. Chem. Phys.* **2019**, *230*, 122–130. [[CrossRef](#)]
39. Song, Y.L.; Dou, Z.H.; Zhang, T.A.; Liu, Y. Research Progress on the Extractive Metallurgy of Titanium and Its Alloys. *Miner. Process. Extr. Metall. Rev.* **2020**, *42*, 535–551.
40. Choi, K.; Choi, H.; Sohn, I. Understanding the magnesiothermic reduction mechanism of TiO₂ to produce Ti. *Metall. Mater. Trans. B* **2017**, *48*, 922–932.
41. Zhao, K.; Wang, Y.W.; Feng, N.X. Cleaner production of Ti powder by a two-stage aluminothermic reduction process. *JOM* **2017**, *69*, 1795–1800.

Disclaimer/Publisher’s Note: The statements, opinions and data contained in all publications are solely those of the individual author(s) and contributor(s) and not of MDPI and/or the editor(s). MDPI and/or the editor(s) disclaim responsibility for any injury to people or property resulting from any ideas, methods, instructions or products referred to in the content.